applied optics

Calibration of line-scan cameras for precision measurement

Bo Sun, Jigui Zhu, Linghui Yang,* Shourui Yang, and Zhiyuan Niu

State Key Laboratory of Precision Measuring Technology and Instruments, Tianjin University, Tianjin 300072, China
*Corresponding author: yanglh.tju@gmail.com

Received 7 April 2016; revised 25 July 2016; accepted 3 August 2016; posted 3 August 2016 (Doc. ID 262735); published 23 August 2016

Calibration of line-scan cameras for precision measurement should have large calibration volume and be flexible in the actual measurement field. In this paper, we present a high-precision calibration method. Instead of using a large 3D pattern, we use a small planar pattern and a precalibrated matrix camera to obtain plenty of points with a suitable distribution, which would ensure the precision of the calibration results. The matrix camera removes the necessity of precise adjustment and movement and links the line-scan camera to the world easily, both of which enhance flexibility in the measurement field. The method has been verified by experiments. The experimental results demonstrated that the proposed method gives a practical solution to calibrate line scan cameras for precision measurement.

OCIS codes: (150.1488) Calibration; (040.1490) Cameras; (120.0120) Instrumentation, measurement, and metrology.

http://dx.doi.org/10.1364/AO.55.006836

1. INTRODUCTION

Line-scan cameras, as one-dimensional imaging devices, have characteristics of high resolution and high frame rate. These characteristics provide new possibilities for measurement of high-speed continuous moving objects with higher accuracy. Therefore, line-scan cameras have been widely used in vision measurement instead of matrix cameras, especially in real-time applications.

Calibration is a necessary process when cameras are used for precision measurement, such as in industrial optical metrology. The quality of calibration has a significant impact on measurement results. Calibration of matrix cameras is one of the most active research areas in both computer vision and photogrammetry. Much effort has been made to facilitate the calibration procedure [1,2]. Unfortunately, the methods cannot be directly used for line-scan cameras. On the other hand, the research of line-scan camera calibration is not as popular as matrix camera calibration. Several research projects on line-scan camera calibration have been done in the last decades. However, only a few calibration methods have been proposed, which is far from the state of the art. The methods found in the literature can be grouped into static calibration and scanning calibration.

In static calibration, patterns used for matrix camera calibration are not available because line-scan cameras cannot tell where a given point in 3D space will be projected into the camera. Thus static calibration methods usually utilize patterns consisting of several feature lines. The intersection points of the camera's viewing plane with the feature lines are used for calibration. Coordinates of these intersection points are calculated according to pattern geometry, based on the principle of cross-ratio invariance. Horaud was the first to propose this kind of calibration method [3]. The approach is easy to implement due to its simplicity; however, the pattern must translate along the Y or Z axis with known increments. The results of the calibration depend on the precision of the displacements. To overcome this limitation, more practical methods are proposed in [4,5]. 3D patterns with multiple planes are employed. A single capture is enough to estimate the parameters. It is therefore not necessary to change the position of the pattern during calibration. Compared with Horaud's method, these methods are easier and more flexible for use. However, these methods are restricted to scant space points and small calibration volume because the size of the pattern is limited, which has a negative influence on the parameters. Although a large pattern is helpful, it is expensive to manufacture and difficult to handle and transport, especially in the actual measurement field. Therefore, static calibration still cannot fulfill the demands of precision measurement, especially when the lens has a large distortion.

Scanning calibration is another type of calibration method. Drareni outlines a novel method to estimate the parameters of line-scan cameras using a planar grid pattern [6]. The pattern moves with a constant velocity relative to the camera, resulting in a 2D image. The correspondences between the points on the pattern and the image points are determined directly. The advantage of this method is that the algorithm is linear and simple, since the parameters are solved by a series of matrix operations

after obtaining the image coordinates by a simple center-extraction algorithm. The major drawback is that the target's motion must be orthogonal to the camera's orientation, which is difficult to achieve. Hui presents a series of scanning calibration methods using 3D patterns instead of planar patterns [7–9]. Compared with static calibration methods, scanning calibration methods employ more points, which would contribute to the precision of the parameters. However, scanning calibration is not usually permitted in the measurement field, because it is difficult to provide a pure linear motion for the pattern under the actual measurement conditions, where there are many restrictions on experimental arrangements.

The general aim of our research is to provide a calibration method of line-scan cameras for precision measurement. In this paper, we use a purposely designed planar pattern that is easy to transport and to use. Meanwhile, a matrix camera is used. With the help of the matrix camera, we can move the pattern freely and obtain a large number of intersection points with a suitable distribution, which results in an increase in precision. The method works without precise adjustment and movement and the obtained parameters are with respect to the world coordinate frame directly. These characteristics would facilitate the experiment in the actual measurement field.

The remainder of the paper is organized as follows: Section 2 describes the mathematical model for line-scan cameras. Section 3 presents the proposed calibration method that consists of two parts: obtaining the point correspondences and estimating the parameters. The experiments and results are reported in Section 4. Finally, conclusions are summarized in Section 5.

2. MATHEMATICAL MODEL FOR THE LINE-SCAN CAMERA

A model that maps a space point to an image point is necessary for calibrating a line-scan camera. A line-scan camera can be regarded as a special camera that consists of only one array of pixels at the center position. Central projection is satisfied only along the pixel array direction. The projection center and the pixel array define the viewing plane. The camera can only see objects in this plane. A point $\boldsymbol{P}(X^w, Y^w, Z^w)$ in the viewing plane projects onto the pixel array at point $\boldsymbol{p}(0, v)$, which is described as a projection matrix $\boldsymbol{M}$:

$$\begin{bmatrix} 0 \\ v \\ 1 \end{bmatrix} \propto \boldsymbol{M} \begin{bmatrix} X^w \\ Y^w \\ Z^w \\ 1 \end{bmatrix}. \tag{1}$$

The matrix $\boldsymbol{M}$ can be further decomposed as follows:

$$\boldsymbol{M} = \begin{bmatrix} 1 & 0 & 0 & 0 \\ 0 & F_y & v_c & 0 \\ 0 & 0 & 1 & 0 \end{bmatrix} \begin{bmatrix} \boldsymbol{R} & \boldsymbol{T} \\ 0 & 1 \end{bmatrix}, \tag{2}$$

where v_c and F_y are, respectively, the principal point and the focal length of the line-scan camera. The matrix $\boldsymbol{R}$ and vector $\boldsymbol{T}$ describe the rigid transformation from the world coordinate frame to the camera coordinate frame.

Furthermore, lens distortion should be included in the camera model for precision measurement. The lens distortion of line-scan cameras exists only in the central projection direction, and it is negligible in the other direction due to the fact that the distance from the principal point (the center of the radial distortion) to the pixel array is too small. We take into account two-order radial distortion and the tangential distortion [10,11]:

$$\Delta v = k_1(v - v_c)^5 + k_2(v - v_c)^3 + k_3(v - v_c)^2, \tag{3}$$

where k_1, k_2, k_3 are the distortion coefficients. By substituting Eqs. (2) and (3) into Eq. (1), we describe the camera model as follows:

$$\begin{cases} 0 = r_{11}X^w + r_{12}Y^w + r_{13}Z^w + t_1 \\ v = v_c + \Delta v + F_y \frac{r_{21}X^w + r_{22}Y^w + r_{23}Z^w + t_2}{r_{31}X^w + r_{32}Y^w + r_{33}Z^w + t_3}, \end{cases} \tag{4}$$

where r_{ij} are the entries of the rotation matrix $\boldsymbol{R}$ and t_1, t_2, t_3 are the components of the translation vector $\boldsymbol{T}$. In Eq. (4), the first part is the equation of the viewing plane and the second part represents the central projection.

The rotation matrix $\boldsymbol{R}$ can be parameterized by a vector $(r_1, r_2, r_3)^T$ according to the Rodrigues formula, which is parallel to the rotation axis and whose magnitude is equal to the rotation angle. Therefore, there are 11 pending parameters for a line-scan camera, in which five parameters (v_c, F_y, k_1, k_2, k_3) are the intrinsic parameters, and six parameters (r_1, r_2, r_3, t_1, t_2, t_3) are the extrinsic parameters.

3. PROPOSED CALIBRATION METHOD

A. Obtaining the Point Correspondences

The key issue in line-scan camera calibration is how the correspondences between space points and image points are established. A planar pattern is used in our method. As illustrated in Fig. 1, five vertical lines ($\boldsymbol{l}_1$, $\boldsymbol{l}_3$, $\boldsymbol{l}_5$, $\boldsymbol{l}_7$, $\boldsymbol{l}_9$) and four diagonal lines ($\boldsymbol{l}_2$, $\boldsymbol{l}_4$, $\boldsymbol{l}_6$, $\boldsymbol{l}_8$) are drawn, combined with a grid of reference points. To eliminate the effect of perspective eccentricity, ring markers are used instead of solid circular markers. Therefore, a more accurate measurement can be obtained when the target plane is not parallel with the camera, as described in [12]. The pattern coordinate frame is defined where the bottom left ring serves as the origin, the X axis is identical to the horizontal line, the Y axis is identical to the vertical line, and the Z

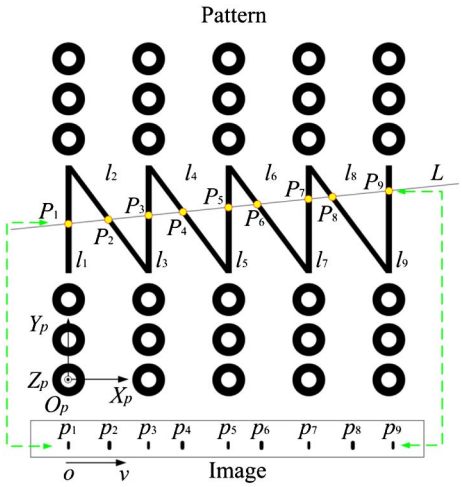

Fig. 1. Calibration pattern comprising five vertical lines, four diagonal lines, and several reference points.

axis is perpendicular to the pattern plane. The equations of the feature lines and the coordinates of the reference points are known in the pattern coordinate frame. By customizing the line width and the ring's diameter, we can locate the lines and rings accurately, even in a blurry image when the pattern is out of depth of field.

The line $\boldsymbol{L}$ is the viewing line of the line-scan camera. It intersects with the feature lines $\boldsymbol{l}_i$ at the points $\boldsymbol{P}_i$. The intersection points project onto the pixel array, resulting in the image points $\boldsymbol{p}_i$. With the image coordinates $\boldsymbol{v}_i$ of the image points and the pattern geometry, we can obtain the coordinates of the corresponding points $\boldsymbol{P}_i$ by the following method.

According to pattern geometry, the Z coordinate is always zero with respect to the pattern coordinate frame and the equations of the vertical lines are as follows:

$$\begin{cases} \boldsymbol{l}_1{:}x = a_1 \\ \boldsymbol{l}_3{:}x = a_3 \\ \boldsymbol{l}_5{:}x = a_5 \\ \boldsymbol{l}_7{:}x = a_7 \\ \boldsymbol{l}_9{:}x = a_9 \end{cases}. \tag{5}$$

The equations of the diagonal lines are

$$\begin{cases} \boldsymbol{l}_2{:}y = k_2x + b_2 \\ \boldsymbol{l}_4{:}y = k_4x + b_4 \\ \boldsymbol{l}_6{:}y = k_6x + b_6 \\ \boldsymbol{l}_8{:}y = k_8x + b_8 \end{cases}. \tag{6}$$

The X coordinates of the intersection points on the vertical lines are known as

$$\begin{cases} X_1 = a_1 \\ X_3 = a_3 \\ X_5 = a_5 \\ X_7 = a_7 \\ X_9 = a_9 \end{cases}. \tag{7}$$

To get the X coordinates of the intersection points on the diagonal lines, we use the cross-ratio of collinear points, which is invariant under central projection. The cross-ratio of four points on the viewing line satisfies

$$\lambda = \frac{\overline{\boldsymbol{P}_d\boldsymbol{P}_n}\cdot\overline{\boldsymbol{P}_l\boldsymbol{P}_m}}{\overline{\boldsymbol{P}_l\boldsymbol{P}_n}\cdot\overline{\boldsymbol{P}_d\boldsymbol{P}_m}} = \frac{\overline{\boldsymbol{p}_d\boldsymbol{p}_n}\cdot\overline{\boldsymbol{p}_l\boldsymbol{p}_m}}{\overline{\boldsymbol{p}_l\boldsymbol{p}_n}\cdot\overline{\boldsymbol{p}_d\boldsymbol{p}_m}}, \tag{8}$$

where $\boldsymbol{P}_d$ $(d = 2, 4, 6, 8)$ subjects to the diagonal lines and $\boldsymbol{P}_l$, $\boldsymbol{P}_m$, $\boldsymbol{P}_n$ are three arbitrary intersection points on the vertical lines, and $\boldsymbol{p}_d$, $\boldsymbol{p}_l$, $\boldsymbol{p}_m$, $\boldsymbol{p}_n$ are their corresponding image points.

Because the coordinates of the image points can be measured in the image, λ can be calculated directly. According to Eq. (8), we can obtain the X coordinate of $\boldsymbol{P}_d$ $(d = 2, 4, 6, 8)$:

$$X_d = \frac{\lambda a_m(a_l - a_n) - a_n(a_l - a_m)}{\lambda(a_l - a_n) - (a_l - a_m)}. \tag{9}$$

Here, for one diagonal line, we can select three arbitrary ones from the total of five vertical lines to compute the cross-ratio. However, considering the effects of the distortion, we select the nearest ones such that the measurement errors on the detection of the lines can be compensated. Therefore, the distortion has no considerable influence.

The Y coordinate of $\boldsymbol{P}_d$ $(d = 2, 4, 6, 8)$ can be computed according to the equation of $\boldsymbol{l}_d$ $(d = 2, 4, 6, 8)$:

$$Y_d = k_dX_d + b_d. \tag{10}$$

After obtaining all the coordinates of the intersection points on the diagonal lines, we compute the equation of the viewing line. Here we define the viewing line by

$$\boldsymbol{L}{:}Y = KX + B. \tag{11}$$

The coefficients can be estimated via the least square method:

$$[K \quad B]^T = (\boldsymbol{A}^T\boldsymbol{A})^{-1}\boldsymbol{A}^T\boldsymbol{b}, \tag{12}$$

where

$$A = \begin{bmatrix} X_2 & 1 \\ X_4 & 1 \\ X_6 & 1 \\ X_8 & 1 \end{bmatrix} b = \begin{bmatrix} Y_2 \\ Y_4 \\ Y_6 \\ Y_8 \end{bmatrix}.$$

Then the Y coordinate of the intersection points $\boldsymbol{P}_v$ $(v = 1, 3, 5, 7, 9)$ on the vertical lines is also computed by

$$Y_v = Ka_v + B. \tag{13}$$

Using this method, we have all the coordinates of the intersection points with respect to the pattern coordinate frame, which are noted by $[X_i, Y_i, 0\ (i = 1, 2, \ldots, 9)]$.

In order to determine the parameters uniquely, we have to move the pattern to multiple positions with respect to the camera. In general, two positions would be sufficient to realize the approach, which is the situation of the method proposed in [4]. But for the stability and accuracy of the method, we should offer more points in depth that ensure that parameters are easier to determine and have smaller correlations [13].

On the other hand, the number and distribution of the image points are of major importance for an accurate determination of distortion parameters. The image sequence for camera calibration should be arranged in such a way that, within the full set of images, use of the complete image format is achieved. Only then is it possible to determine distortion parameters that are valid across this whole format.

Based on the above statements, the pattern is moved to various positions in the object space during calibration, as illustrated in Fig. 2. All the points on the pattern of different positions must subsequently be transformed into a common coordinate system. A matrix camera is therefore used to aid the calibration process. In each position, the matrix camera captures the pattern synchronously with the line-scan camera by an external trigger. After image acquisition, we place the pattern to another position. Repeat this process until a suitable distribution of the points is achieved. To obtain the transformation from the pattern to the matrix camera, the calibration algorithm proposed by Zhang (see [1]) is applied to calculate the extrinsic parameters of the matrix camera relative to the pattern coordinate system. In general, we usually calibrate the matrix camera in lab previously and lock the focus and aperture settings of the lens so that the intrinsic parameters are constant and available for the following procedure. Therefore, we can achieve the pattern's position and orientation with a single shot. Furthermore, the distortions can be corrected, so we can still ensure the accuracy of the pattern's position and orientation with a small pattern in the measurement field. It is important because a large pattern is difficult to transport and hard to use

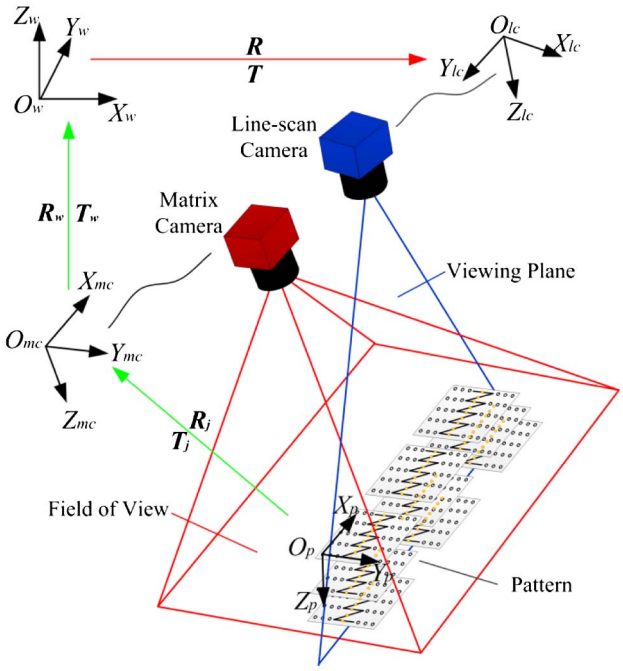

Fig. 2. General view of our calibration method. $O_wX_wY_wZ_w$ is the world coordinate system. $O_{lc}X_{lc}Y_{lc}Z_{lc}$ and $O_{mc}X_{mc}Y_{mc}Z_{mc}$ denote the coordinate system of the line-scan camera and the matrix camera, respectively. $O_pX_pY_pZ_p$ represents the pattern coordinate system.

in the measurement field. According to the extrinsic parameters, we obtain the transformation in each position, which is noted by $\{\boldsymbol{R}_j,\ \boldsymbol{T}_j\ (j = 1, 2, \ldots, n)\}$ at the *j-th* position.

In order to establish the transformation from the matrix camera to the world coordinate frame, the matrix camera should measure the reference points that define the world coordinate frame of the actual measurement field. This transformation is denoted by $\{\boldsymbol{R}_w, \boldsymbol{T}_w\}$. After a series of rigid transformations, all the points are aligned to the world coordinate frame. The coordinates of the points in the world coordinate frame are described as

$$\begin{bmatrix} X^w_{i,j} \\ Y^w_{i,j} \\ Z^w_{i,j} \end{bmatrix} = \boldsymbol{R}_w \cdot \left(\boldsymbol{R}_j \begin{bmatrix} X_{i,j} \\ Y_{i,j} \\ 0 \end{bmatrix} + \boldsymbol{T}_j \right) + \boldsymbol{T}_w (i = 1, 2 \ldots 13, j = 1, 2, \ldots n), \quad \textbf{(14)}$$

where the subscript i means the line number and the subscript j is the position number.

It is worth noting that the calibration errors of the matrix camera would transform into the calibration of the line-scan camera. It is instructive to consider the errors introduced from the matrix camera. Calibration error of the matrix camera will bring errors to the world coordinates of the space points that affect the determination of the parameters directly. Therefore, it is recommended that the matrix camera should be calibrated previously in the laboratory with high accuracy. Fortunately, there are various techniques to calibrate matrix cameras, such as plane-based calibration (proposed by Zhang in [1]), test-field calibration, and self-calibration [13]. Of course, more space points with a good distribution should be provided for an accurate calibration. In addition, a higher resolution is helpful, and the frame-rate can be very low because of static imaging. Therefore, an economical high-resolution and low-rate camera is suitable for our method.

In brief, the procedure for the point correspondences can be summarized by the following steps:

1. Determine the X coordinate of the intersection points on the diagonal lines according to cross-ratio invariance.
2. Compute the Y coordinate of the intersection points on the diagonal lines according to the pattern geometry.
3. Obtain the equation of the viewing line.
4. Compute the Y coordinate of the intersection points on the vertical lines.
5. Align the points to the world coordinate frame by the matrix camera.
6. Move the pattern to another place and repeat step 1 to step 5 until a suitable distribution of the points is achieved.

Finally, the pattern is placed in n positions during calibration. Therefore, we have N $(N = 9n)$ points in total in the world coordinate frame.

B. Estimating the Parameters

With a set of points in the world coordinate frame and their corresponding projections, the camera parameters can be calculated by a two-step calibration method. The first step is to obtain the initial guess of the parameters, and then a nonlinear optimization is performed to refine the parameters.

1. Obtaining Initial Values

Expanding Eq. (2), we take the last two rows

$$\begin{bmatrix} \boldsymbol{m}_2 & m_{24} \\ \boldsymbol{m}_3 & m_{34} \end{bmatrix} = \begin{bmatrix} F_y \boldsymbol{r}_2 + v_c \boldsymbol{r}_3 & F_y t_2 + v_c t_3 \\ \boldsymbol{r}_3 & t_3 \end{bmatrix}, \quad \textbf{(15)}$$

where $\boldsymbol{m}_2 = [m_{21}, m_{22}, m_{23}]$, $\boldsymbol{m}_3 = [m_{31}, m_{32}, m_{33}]$, and $\boldsymbol{r}_2$ and $\boldsymbol{r}_3$ are the row vectors of the rotation matrix $\boldsymbol{R}$. Obviously, the elements of $\boldsymbol{m}_3$ satisfy the constraint $m_{31}^2 + m_{32}^2 + m_{33}^2 = 1$.

The parameters can be extracted from the matrix $\boldsymbol{M}$ according to Eqs. (4) and (15) as follows:

$$\begin{cases} v_c = \boldsymbol{m}_2 \cdot \boldsymbol{m}_3 \\ F_y = \|\boldsymbol{m}_2 \times \boldsymbol{m}_3\| \\ \boldsymbol{r}_2 = (\boldsymbol{m}_2 - v_c \boldsymbol{m}_3)/F_y \\ \boldsymbol{r}_3 = \boldsymbol{m}_3 \\ \boldsymbol{r}_1 = \boldsymbol{r}_2 \times \boldsymbol{r}_3 \\ t_2 = (m_{24} - v_c m_{34})/F_y \\ t_3 = m_{34} \\ t_1 = \frac{1}{N} \sum_{i=1}^{N} (-\boldsymbol{r}_1 \boldsymbol{P}_i^{\boldsymbol{W}}) \end{cases}. \quad \textbf{(16)}$$

We can also obtain the camera's projection center with respect to the world coordinate frame:

$$\begin{bmatrix} O_1 \\ O_2 \\ O_3 \end{bmatrix} = -\boldsymbol{R} \begin{bmatrix} t_1 \\ t_2 \\ t_3 \end{bmatrix}. \quad \textbf{(17)}$$

So, the crux of the problem is to estimate the projection matrix $\boldsymbol{M}$. For each correspondence, we have a linear equation according to Eq. (1). Given N points from the method of Section 3.A, we get an overdetermined system:

$$\begin{bmatrix} X_1^w & Y_1^w & Z_1^w & 1 & -v_1X_1^w & -v_1Y_1^w & -v_1Z_1^w & v_1 \\ \vdots & \vdots & \vdots & \vdots & \vdots & \vdots & \vdots & \vdots \\ X_N^w & Y_N^w & Z_N^w & 1 & -v_NX_N^w & -v_NY_N^w & -v_NZ_N^w & v_N \end{bmatrix} \begin{bmatrix} m_{21} \\ m_{22} \\ m_{23} \\ m_{24} \\ m_{31} \\ m_{32} \\ m_{33} \\ m_{34} \end{bmatrix} = 0. \tag{18}$$

The parameters can be solved via a closed-form solution that is used in the classical calibration method proposed in [14]. However, errors exist in both the world coordinates and the image coordinates, especially in the world coordinates, because they are not extracted from the pattern directly but derived from the image coordinates. Therefore, the parameters are very sensitive to the errors of the image points. It is necessary to make a better estimation of the parameters. So the constraint $m_{31}^2 + m_{32}^2 + m_{33}^2 = 1$ is involved. Rewriting Eq. (18), we have

$$\begin{cases} \boldsymbol{C}_3\boldsymbol{\varphi}_3 + \boldsymbol{C}_5\boldsymbol{\varphi}_5 = 0 \\ \boldsymbol{\varphi}_3 = 1 \end{cases}, \tag{19}$$

where

$$\boldsymbol{C}_3 = \begin{bmatrix} -v_1X_1^w & -v_1Y_1^w & -v_1Z_1^w \\ \vdots & \vdots & \vdots \\ -v_NX_N^w & -v_NY_N^w & -v_NZ_N^w \end{bmatrix}$$

$$\boldsymbol{C}_5 = \begin{bmatrix} X_1^w & Y_1^w & Z_1^w & 1 & v_1 \\ \vdots & \vdots & \vdots & \vdots & \vdots \\ X_N^w & Y_N^w & Z_N^w & 1 & v_N \end{bmatrix}$$

$$\boldsymbol{\varphi}_3 = [m_{31} \quad m_{32} \quad m_{33}]^T$$

$$\boldsymbol{\varphi}_5 = [m_{21} \quad m_{22} \quad m_{23} \quad m_{24} \quad m_{34}]^T.$$

According to Eq. (19), the objective function to be minimized is

$$f(\boldsymbol{\varphi}_3, \boldsymbol{\varphi}_5) = \|\boldsymbol{C}_3\boldsymbol{\varphi}_3 + \boldsymbol{C}_5\boldsymbol{\varphi}_5\|^2 + \mu(\|\boldsymbol{\varphi}_3\|^2 - 1), \tag{20}$$

where μ is the Lagrange multiplier. In order to get the minimum value of the objective function, we compute the partial derivatives of φ_3 and φ_5, respectively, and make them be equal to 0:

$$\begin{cases} \frac{\partial f}{\partial \boldsymbol{\varphi}_3} = 2\boldsymbol{C}_3^T\boldsymbol{C}_3\boldsymbol{\varphi}_3 + 2\boldsymbol{C}_3^T\boldsymbol{C}_5\boldsymbol{\varphi}_5 + 2\mu\boldsymbol{\varphi}_3 = 0 \\ \frac{\partial f}{\partial \boldsymbol{\varphi}_5} = 2\boldsymbol{C}_5^T\boldsymbol{C}_5\boldsymbol{\varphi}_5 + 2\boldsymbol{C}_5^T\boldsymbol{C}_3\boldsymbol{\varphi}_3 = 0 \end{cases}. \tag{21}$$

Solving the equations in Eq. (21), we obtain

$$\begin{cases} \boldsymbol{D}\boldsymbol{\varphi}_3 = \mu\boldsymbol{\varphi}_3 \\ \boldsymbol{\varphi}_5 = -(\boldsymbol{C}_5^T\boldsymbol{C}_5)^{-1}\boldsymbol{C}_5^T\boldsymbol{C}_3\boldsymbol{\varphi}_3 \end{cases}, \tag{22}$$

where

$$\boldsymbol{D} = -\boldsymbol{C}_3^T\boldsymbol{C}_3 + \boldsymbol{C}_3^T\boldsymbol{C}_5(\boldsymbol{C}_5^T\boldsymbol{C}_5)^{-1}\boldsymbol{C}_5^T\boldsymbol{C}_3.$$

Obviously, φ_3 is the eigenvector of the matrix $\boldsymbol{D}$. Note that there are three eigenvectors for the matrix $\boldsymbol{D}$, and thus there are three groups of parameters. We project the points according to each group of parameters to get the derived image points. The differences between the true image points and the derived values are reprojection errors. We choose the one with the fewest reprojection errors as the solution. Furthermore, we must guarantee that $m_{34}(m_{34} = t_3)$ is positive because the pattern is always in front of the camera.

Once $\boldsymbol{\varphi}_3$ and $\boldsymbol{\varphi}_5$ are obtained, the projection matrix $\boldsymbol{M}$ is known. The initial values of the parameters, except the distortion coefficients, are extracted according to Eq. (16). The initial values of the distortion coefficients are set to zero because the distortion is usually small.

2. Nonlinear Optimization

In the initial estimation of the parameters, the distortion is neglected while obtaining the intersection points, which would cause errors in the image points. In addition, the intersection points are calculated according to the image points. So the intersection points would be further affected and the obtained intersection points are therefore not the true space points corresponding to the image points. Therefore, it is necessary to further refine the parameters via a nonlinear optimization.

In the optimization process, the distortion is included. On the other hand, we recompute the intersection points for each iteration by the current viewing plane and the pattern geometry, instead of using the cross-ratio invariance of the image points.

Once an initial estimation of the parameters has been carried out, an optimization procedure can be applied in order to minimize the reprojection error and be represented by the following objective function:

$$f(\boldsymbol{\varphi}) = \sum_{k=1}^{N} \|v_k - rep.v_k(\varphi, l_k)\|^2, \tag{23}$$

where $\varphi = (v_c, F_y, r_1, r_2, r_3, t_1, t_2, t_3, k_1, k_2, k_3)$ and l_k is the feature line corresponding to the *k-th* point. v_k is the image coordinate extracted from the actual image. $rep.v_k$ is the image coordinate reprojected by the current viewing plane and the pattern geometry.

4. EXPERIMENTS

We have tested the proposed algorithm using a Dalsa Spyder3 line-scan camera of 4096 pixels, with a pixel size of 10 μm and a focal length of 50 mm. In order to ensure accuracy, we use a glass calibration target with a photolithographic pattern. The size of the pattern is 152 mm × 152 mm (Fig. 3). The accuracy of the pattern is better than 1 μm, and the flatness of glass is less than 5 μm. The pattern is illuminated by an LED array (wavelength: 455 nm) to ensure the detection of the intersection points with subpixel accuracy. The matrix camera used is an Imperx Bobcat B3320 with a 25 mm lens. The external trigger output of the matrix camera serves as the frame trigger of the line-scan camera to synchronize image acquisition.

The images were acquired at a line rate of 1000 Hz via a GigE interface. Two hundred lines for each image were taken to reduce noise introduced during the image acquisition. The average values were used for the calibration algorithm. All the algorithms were implemented in MATLAB on a PC (with a Core i5 CPU). For simplicity, we set the matrix camera coordinate system as the world coordinate system, so the rotation

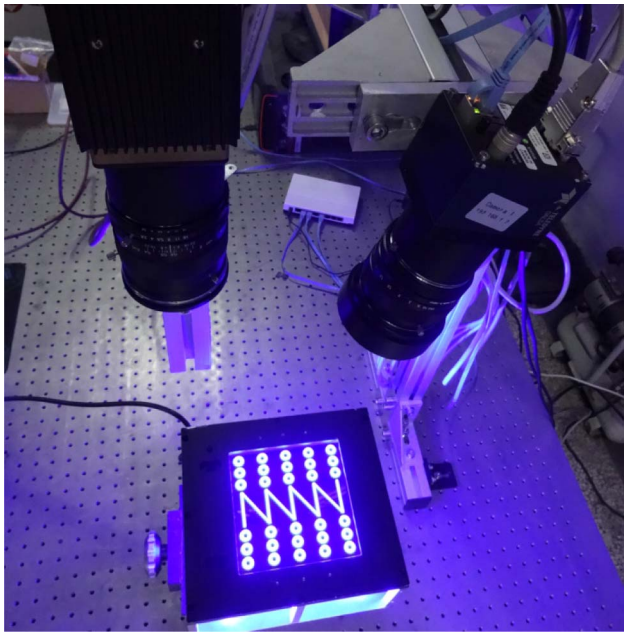

Fig. 3. Experimental setup to verify our calibration method. The right camera is the line-scan camera to be calibrated and the other is a matrix camera whose parameters are known.

from the matrix camera to the world $\boldsymbol{R}_w$ is an identity matrix and the translation $\boldsymbol{T}_w$ is a zero vector.

We placed the pattern to fifteen positions during calibration. The images captured by the line-scan camera and matrix camera are shown in Figs. 4 and 5, respectively. The images are labeled with their corresponding position numbers. In Fig. 4, it is clear that the image points fill the complete image format.

Positions of the intersection points were extracted from the line-scan images by a subpixel algorithm. The positions and orientations of the pattern were measured by the matrix camera based on the images in Fig. 5. The results are recorded in Table 1, where the orientations are expressed as rotation vectors according to the Rodrigues formula.

In Table 1, the range in the Z direction is about 160 mm, which almost reaches the limit of the depth of field of the line-scan camera. We project the rings to the camera using the parameters listed in Table 1 to calculate the reprojection error, and the average value is 0.06 pixel.

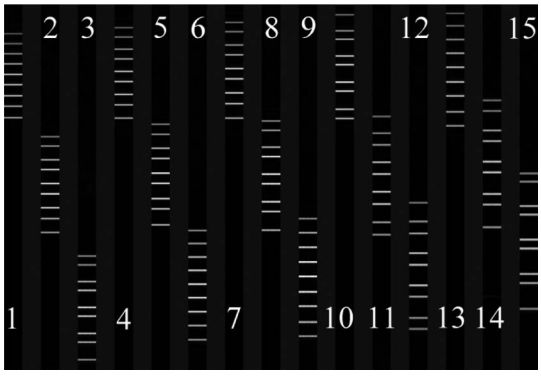

Fig. 4. Images captured by the line-scan camera.

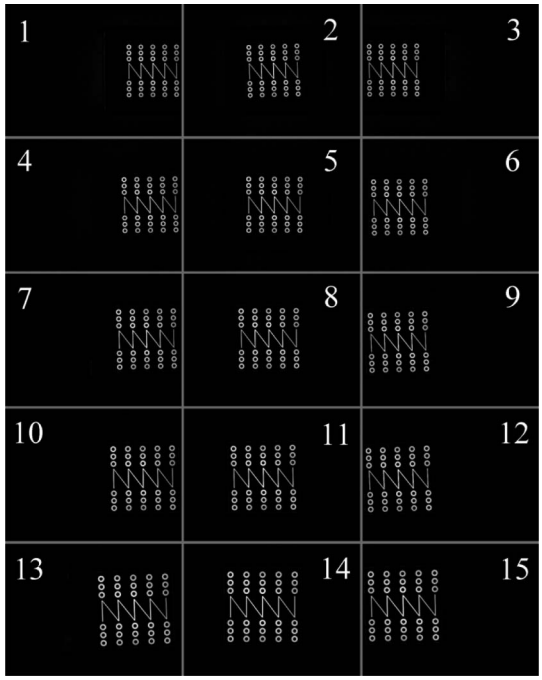

Fig. 5. Images captured by the matrix camera.

According the positions and orientations of the pattern together with the image points, we obtained 135 points in total, whose distribution is shown in Fig. 6.

Then, we used all the points to estimate the parameters. The calculation terminated after 421 iterations, costing 27.315 s. The initial values and final results are listed in Table 2. The reprojection errors are shown in Fig. 7. We can see clearly that the initial values of the parameters are quite close to the final values (Table 2). The reprojection errors improve significantly through the nonlinear optimization (Fig. 7). After the optimization, the maximum value of the reprojection errors is 0.42 pixel and the root mean square value is 0.10 pixel.

In order to further investigate the performance of the proposed method, we divided the points into five groups according

Table 1. Positions and Orientations of the Pattern

Rotation Vectors (rad)			Positions (mm)		
r_1	r_2	r_3	T_x	T_y	T_z
−3.1267	0.0097	−0.0051	80.075	−65.308	634.917
−3.1269	0.0445	−0.0038	−66.584	−64.432	634.693
−3.1274	0.0107	−0.0011	−213.463	−67.076	634.521
−3.1328	−0.0251	−0.0341	64.080	−66.865	598.003
−3.1011	−0.0011	−0.0419	−62.366	−67.402	591.982
−3.1232	0.0200	−0.0781	−188.665	−61.320	592.082
−3.1264	0.0331	−0.0016	47.627	−67.410	554.866
−3.1268	0.0125	−0.0026	−74.930	−69.294	554.491
−3.1266	0.0451	0.0001	−183.938	−60.073	554.543
−3.1258	0.0271	0.0312	33.315	−58.366	517.913
−3.1266	0.0251	0.0325	−85.504	−59.409	517.760
−3.1255	0.0556	0.0345	−175.595	−55.320	517.717
−3.1261	0.0614	−0.0012	8.040	−63.198	474.618
−3.1242	−0.0019	−0.0036	−84.107	−71.190	474.170
−3.1231	0.0283	−0.0028	−156.407	−72.079	473.998

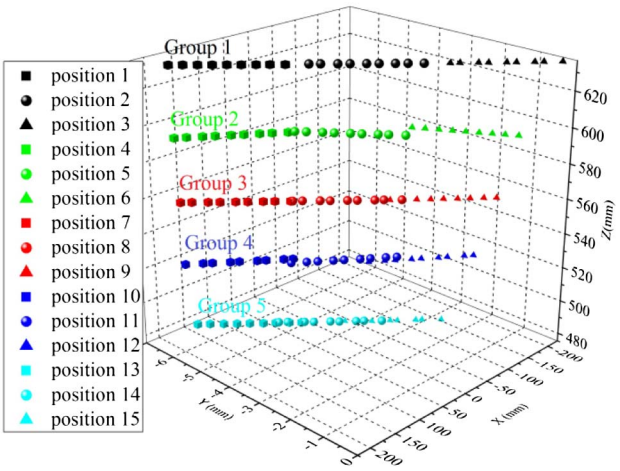

Fig. 6. Distribution of the points, which are divided into five groups according to their depths, displayed with different colors.

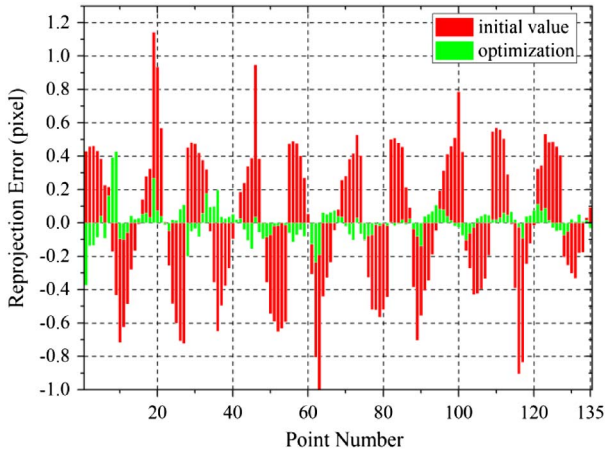

Fig. 7. Reprojection errors for all the points.

Table 2. Calibration Result with All Points

Parameters (unit)	Initial Values	Final Values
v_c (pixel)	2035.49	2012.80
F_y (pixel)	5528.58	5556.15
r_1 (rad)	0.194698	0.196206
r_2 (rad)	−0.181720	−0.185599
r_3 (rad)	1.575995	1.574717
O_1 (mm)	−154.812	−155.151
O_2 (mm)	−7.351	−6.677
O_3 (mm)	26.929	24.133
k_1 (10^{-17})	0	−1.12
k_2 (10^{-10})	0	1.57
k_3 (10^{-8})	0	−1.49
RMS (pixel)	0.42	0.10

to depth, which were labeled Group 1 to 5 (see Fig. 6). We applied our calibration algorithm to all the combinations of two (similar to the configuration in [4]), three, and four groups. The results are shown in Table 3. For each configuration, two columns are given. The first column is the mean value and the second column is the deviation, representing the precision of the parameters. The last row indicates the root mean square of the reprojection errors.

We can see from Tables 2 and 3 that the results are very consistent with each other, whether we used two, three, four, or five groups. However, as is clear, the deviation decreases with the number of groups, which means a higher precision and also means that the result is more reliable. We also note that the distortion coefficients are quite stable, because the points covered the complete image format in all configurations. The deviation of the focal length is larger when fewer groups are used. This is primarily due to the fact that the depth distribution of the points varies considerably among the combinations of the groups.

5. CONCLUSION

In this paper, we have presented a high-precision method to calibrate a line-scan camera. A planar pattern with a customized geometry is utilized to establish the correspondence between the image points and the space points. The method requires the pattern to move to different positions. The position and orientation of the pattern are measured and transformed to the world coordinate frame by a matrix camera. The proposed method has been verified by real data, and very good results are obtained.

Table 3. Calibration Results with Various Configurations

	2 Groups		3 Groups		4 Groups	
Parameters	Mean	Deviation	Mean	Deviation	Mean	Deviation
v_c (pixel)	2020.81	47.53	2027.04	28.51	2028.97	13.74
F_y (pixel)	5533.90	89.67	5546.06	55.92	5528.85	24.51
r_1 (rad)	0.197108	0.001261	0.196625	0.000910	0.197413	0.000481
r_2 (rad)	−0.183126	0.004385	−0.182276	0.002417	−0.181240	0.003325
r_3 (rad)	1.576176	0.002062	1.575368	0.001416	1.576720	0.000647
O_1 (mm)	−154.699	2.043	−155.201	1.322	−154.867	1.201
O_2 (mm)	−7.726	0.452	−7.821	0.254	−8.379	0.315
O_3 (mm)	26.920	3.418	25.389	2.963	27.295	1.417
k_1 (10^{-17})	−1.23	0.19	−1.09	0.18	−1.21	0.15
k_2 (10^{-10})	1.54	0.23	1.47	0.15	1.63	0.16
k_3 (10^{-8})	−1.52	0.21	−1.45	0.16	−1.39	0.13
RMS (pixel)	0.13	0.07	0.12	0.05	0.12	0.04

Compared with other methods, the essential advantage of our proposed method is that the method can offer more points that cover a large depth range and fill the image format, which would contribute to the precision of the parameters and would ensure a better estimation of the distortion coefficients. In addition, compared with using a large precise 3D pattern such as multiple parallel or orthogonal planes, our method has the further advantage that the pattern is relatively economical, convenient to transport, and easy to handle. Finally, the pattern can move freely, which removes the necessity of the precise adjustment and movement of the pattern, and the matrix camera could link the line-scan camera to the world directly. All of these characteristics are quite helpful for precise calibration of line-scan cameras in the actual measurement field. Although a matrix camera is required, it does not matter, because matrix cameras are widely available and relatively low-cost. Therefore, our proposed calibration method is quite suitable for precision measurement.

Funding. National Science Foundation (NSF) (51405338, 51225505).

Acknowledgment. We thank the Computer Vision Research Group of the California Institute of Technology for the use of their camera calibration toolbox.

REFERENCES

1. Z. Y. Zhang, "A flexible new technique for camera calibration," IEEE Trans. Pattern Anal. Mach. Intell. **22**, 1330–1334 (2000).
2. R. Tsai, "A versatile camera calibration technique for high-accuracy 3D machine vision metrology using off-the-shelf TV cameras and lenses," IEEE J. Robot. Autom. **3**, 323–344 (1987).
3. R. Horaud, R. Mohr, and B. Lorecki, "On single-scanline camera calibration," IEEE Trans. Robot. Autom. **9**, 71–75 (1993).
4. C. A. Luna, M. Mazo, J. L. Lazaro, and J. F. Vazquez, "Calibration of line-scan cameras," IEEE Trans. Instrum. Meas. **59**, 2185–2190 (2010).
5. D. Li, G. Wen, B. W. Hui, S. Qiu, and W. Wang, "Cross-ratio invariant based line scan camera geometric calibration with static linear data," Opt. Lasers Eng. **62**, 119–125 (2014).
6. J. Drareni, S. Roy, and P. Sturm, "Plane-based calibration for linear cameras," Int. J. Comput. Vis. **91**, 146–156 (2011).
7. B. Hui, G. Wen, Z. Zhao, and D. Li, "Line-scan camera calibration in close-range photogrammetry," Opt. Eng. **51**, 053602 (2012).
8. B. Hui, J. Zhong, G. Wen, and D. Li, "Determination of line scan camera parameters via the direct linear transformation," Opt. Eng. **51**, 113201 (2012).
9. B. Hui, G. Wen, P. Zhang, and D. Li, "A novel line scan camera calibration technique with an auxiliary frame camera," IEEE Trans. Instrum. Meas. **62**, 2567–2575 (2013).
10. C. B. Duane, "Close-range camera calibration," Photogramm. Eng. **37**, 855–866 (1971).
11. S. Fang, X. Xia, and Y. Xiao, "A calibration method of lens distortion for line scan cameras," Optik **124**, 6749–6751 (2013).
12. J. S. Kim, P. Gurdjos, and I. S. Kweon, "Geometric and algebraic constraints of projected concentric circles and their applications to camera calibration," IEEE Trans. Pattern Anal. Mach. Intell. **27**, 637–642 (2005).
13. T. Luhmann, S. Robson, S. Kyle, and J. Boehm, *Close-Range Photogrammetry and 3D Imaging* (Walter de Gruyter, 2014), pp. 569–571.
14. O. Faugeras, *Three-Dimensional Computer Vision: A Geometric Viewpoint* (MIT, 1993), pp. 51–66.